



**HAL**  
open science

## Thermodynamics of the L3 (Sponge) Phase in the Flexible Surface Model

John Daicic, Ulf Olsson, Hakan Wennerström, Götz Jerke, Peter Schurtenberger

► **To cite this version:**

John Daicic, Ulf Olsson, Hakan Wennerström, Götz Jerke, Peter Schurtenberger. Thermodynamics of the L3 (Sponge) Phase in the Flexible Surface Model. *Journal de Physique II*, 1995, 5 (2), pp.199-215. 10.1051/jp2:1995123 . jpa-00248148

**HAL Id: jpa-00248148**

**<https://hal.science/jpa-00248148>**

Submitted on 4 Feb 2008

**HAL** is a multi-disciplinary open access archive for the deposit and dissemination of scientific research documents, whether they are published or not. The documents may come from teaching and research institutions in France or abroad, or from public or private research centers.

L'archive ouverte pluridisciplinaire **HAL**, est destinée au dépôt et à la diffusion de documents scientifiques de niveau recherche, publiés ou non, émanant des établissements d'enseignement et de recherche français ou étrangers, des laboratoires publics ou privés.

Classification

Physics Abstracts

82.70 — 64.70

## Thermodynamics of the $L_3$ (Sponge) Phase in the Flexible Surface Model

John Daicic <sup>(1)</sup>, Ulf Olsson <sup>(1)</sup>, Håkan Wennerström <sup>(1)</sup>, Götz Jerke <sup>(2)</sup> and Peter Schurtenberger <sup>(2)</sup>

<sup>(1)</sup> Division of Physical Chemistry 1, Chemical Centre, University of Lund, P.O. Box 124, S-221 00 Lund, Sweden

<sup>(2)</sup> Institut für Polymere, ETH Zentrum, CH-8092 Zürich, Switzerland

(Received 5 August 1994, revised 17 October 1994, accepted 9 November 1994)

**Abstract.** — The thermodynamics of the  $L_3$  (sponge) phase is investigated within the flexible surface model. The well-established leading-order  $\Phi^3$  scaling for the free energy density (where  $\Phi$  is the surfactant volume fraction) requires modification in order to describe the narrow character of the phase and the observed sequence of phase transitions. We find that higher order contributions to the free energy density from the local curvature energy provide a straightforward mechanism to account for these features. The phase equilibria with the dilute solution on one side of the phase and the lamellar phase on the other are evaluated for a model binary (surfactant-solvent) system, and calculated phase diagrams are presented. Experimental evidence in support of the model comes from static light scattering experiments on the pseudo-binary system AOT- $\text{NaNO}_3$ -water. We calculate the forward scattering intensity along chosen dilution lines within the phase using the model, and predict that the scattering intensity varies significantly as we move from one phase boundary to the other at constant  $\Phi$ . The experimental results confirm these predictions, and provide strong evidence in support of the proposed model.

### 1. Introduction

The anomalous isotropic  $L_3$  (or sponge) phase [1] is a fluid consisting of a disordered, bicontinuous multiply-connected surfactant bilayer structure separating two domains of the same solvent. This remarkable phase scatters light, shows flow birefringence and is not highly viscous. A distinguishing feature is the narrow character of the one-phase region, the sponge usually being observed in equilibrium with dilute solution on one side of the single-phase region, and a lamellar ( $L_\alpha$ ) phase on the other.

For an isotropic liquid, the narrowness of the  $L_3$  phase is a unique feature. In our view, any model which attempts a thermodynamic description of this phase must successfully predict this behaviour. Previous theoretical models have proposed various mechanisms leading to the formation of the disordered bilayer structure. Cates *et al.* [2] have suggested that the lamellar to  $L_3$  transition is driven entropically and by fluctuations, and that the bending rigidity of

the bilayer is renormalized on a change of length scale. Porte *et al.* [3] argue alternatively that it is the Gaussian curvature of the bilayer membrane which favours the formation of tubular connections between patches of surfactant, and hence the construction of a sponge-like structure.

Recently, Wennerström and Olsson [4] have argued that there is a generic scaling form for the free energy density of sponge phases and their monolayer analogue, bicontinuous microemulsions, which in principle successfully accounts for the narrow character of these phases. Originally, Porte *et al.* [3] showed how a universal first-order scaling law applies to the free energy density of fluid membrane phases, using scale-invariance considerations. This scaling law,

$$g = a(\Phi/l)^3 \quad (1)$$

where  $l$  is the length of the surfactant, is not sufficient, however, to describe the observed equilibria between the competing phases as described above, because of its monotonic nature. Simply, the phase with the smallest coefficient  $a$  is stable at all concentrations. Wennerström and Olsson [4] therefore proposed that the free energy density has additional terms which become significant at higher surfactant concentrations, so that to next order

$$g = a(\Phi/l)^3 + b(\Phi/l)^5 \quad (2)$$

Typically, the sign of the coefficient  $a$  is *negative* for the sponge phase, for reasons that we shall discuss later in this paper. The important point is that under this condition, it is apparent that the sponge phase will have a finite swelling, as it becomes thermodynamically unstable upon dilution. A positive value for the coefficient  $b$  ensures stability at higher concentrations. We see from the outset that within this picture there is a straightforward mechanism for describing the narrow character of the phase.

The issue now becomes one of providing a quantitative analysis within the scope of the above outline that can map a geometrical description of the disordered multiply-connected bilayer structure to a free energy density of the form given in equation (2). The narrow character of the phase indicates an internal constraint on the free energy of the system. Anderson and co-workers [5, 6] have pointed out that this constraint derives naturally from a consideration of the monolayer curvature energy at the interface with solvent. They derived a relation between the volume fraction of bilayer and the average mean curvature at the monolayer interface  $\langle H \rangle$ , this being, in the limit of weakly curved surfaces and low concentrations,

$$\Phi^2 \approx \gamma l \langle H \rangle \quad (3)$$

The value of the coefficient  $\gamma$  was found by them to be approximately - 2. They then argued that the bending energy plays a dominating role in determining the stability of the phase. In this paper, we shall provide a quantitative analysis following these concepts, the goal being to calculate the phase diagram of a model system which displays the  $L_3$  phase.

In the past, the stability of the sponge phase (and also balanced microemulsions) has been explained by invoking a renormalization of the bending rigidity of the surfactant bilayer (or monolayer). In ACRS (Andelman, Cates, Roux and Safran) theory [7], the "bare" bending modulus  $\kappa_0$  is "softened" on a change of length scale, so that the bending modulus of the "base surface" is given by

$$\kappa = \kappa_0 [1 - \tau \ln(\xi/l)] \quad (4)$$

(and similarly for the saddle-splay constant  $\bar{\kappa}$ ), where  $\xi \propto l/\Phi$  is the characteristic length of the sponge structure, and  $\tau = k_B T/4\pi\kappa_0$ . This in turn leads to a correction to the first-order scaling of the free energy density of the form

$$g = \Phi^3(a + b \ln \Phi) \quad (5)$$

Whilst accounting for the stability of the sponge phase, this model fails to describe its narrow character. Recently, Pieruschka *et al.* [8] have shown from a rigorous variational theory calculation that for a lamellar system the logarithmic renormalization of the bending constants is exactly cancelled by a concomitant change in the area of the so-called “base surface”, and hence no logarithmic term appears in the free energy of that system. This has also been argued to apply qualitatively to all fluid bilayer and monolayer phases by Wennerström and Olsson [4]. In this paper we avoid defining a base surface in the sense of ACRS theory, and thus renormalization of the bending constants is not invoked.

One experimental method previously used to test theoretical models of the L<sub>3</sub> phase is static light scattering. This is because the predicted osmotic compressibility of the system can be related directly to the forward scattering intensity obtained from these experiments. Previously, Porte and co-workers [9, 10] and Roux *et al.* [11] have used results from such experiments to confirm predictions deriving from ACRS theory and equation (5). We too have sought experimental confirmation of the model proposed in this paper using this method. As we shall detail in Section 5, the results of these measurements give strong support to the model which we propose.

## 2. Free Energy of the Sponge Phase

Within the flexible surface model, the surfactant bilayer membrane is considered as an ideal connected geometrical surface composed of two oppositely oriented monolayers, and to a good approximation it is free of edges and bifurcations. The local curvature free energy, expanded to second order, is given by [12, 13]

$$g_c = 2\kappa(H - H_0)^2 + \bar{\kappa}K \quad (6)$$

where  $H$  is the mean curvature,  $H_0$  is the spontaneous mean curvature,  $K$  is the Gaussian curvature, and  $\kappa$  and  $\bar{\kappa}$  are the bending modulus and the saddle splay constant respectively. In the model that we shall employ, these quantities will refer to the monolayers which constitute the bilayer membrane. The total curvature free energy of the bilayer (of total area  $A$ )  $G_c$  is given by a surface integration over the constituent monolayers, so that

$$G_c/A = 2\kappa\langle(H - H_0)^2\rangle + \bar{\kappa}\langle K\rangle \quad (7)$$

The mean curvature term may be decomposed into two contributions,

$$2\kappa\langle(H - H_0)^2\rangle = 2\kappa [\langle(H) - H_0\rangle^2 + \langle(H - \langle H \rangle)^2\rangle] \quad (8)$$

the first term corresponding to the bending free energy of the average mean curvature, and the second to the bending energy of fluctuations.

The second term in equation (7) is the Gaussian curvature contribution to the free energy, which can be related directly to the topology of the surface *via* the Gauss-Bonnet theorem [14]

$$A\langle K\rangle = 2\pi\chi_E \quad (9)$$

where the Euler characteristic  $\chi_E$  is a purely topological quantity.

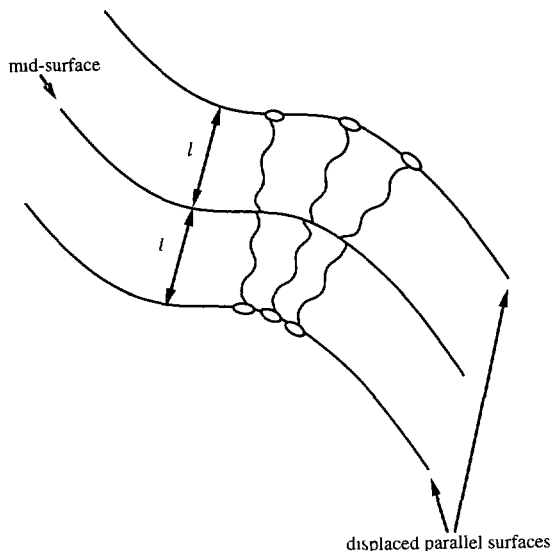


Fig. 1. — Schematic representation of a bilayer cross-section, with bilayer mid-surface at the centre and two displaced parallel surfaces at the interface with solvent.

Now, given a particular configuration of the membrane, the surface over which the integration is performed must be specified. One would prefer to be able to do so at the surfactant-solvent interface. However, the precise identification of this surface remains problematic, and hence we apply the *parallel surfaces model*, where following the assumptions given in reference [5] we consider the bilayer mid-surface as a minimal surface, and perform the integration over two parallel surfaces displaced from the mid-surface by a distance  $l$ , the monolayer thickness. This is illustrated in Figure 1.

The average properties of the displaced parallel surfaces (subscript 1) can be related to those of the mid-surface (m) by [15]

$$\langle H \rangle_1 = \frac{l \langle K \rangle_m}{1 + l^2 \langle K \rangle_m} \quad (10)$$

and

$$\langle K \rangle_1 = \langle K \rangle_m \quad (11)$$

Now, if the spontaneous curvature is towards the solvent, then  $H_0 < 0$ . (We will show later that this is a requirement for the stability of the sponge phase over almost the entire range of concentrations where it appears.) Given this, certain conclusions can be drawn immediately from the preceding equations. Minimizing the curvature energy means that  $\langle H \rangle_1 \approx H_0$ , and in the limit of weakly curved surfaces  $|l^2 \langle K \rangle| \ll 1$ , so that equation (10) implies that  $\langle K \rangle < 0$ . The Gauss-Bonnet theorem given in equation (9) then requires that  $\chi_E$  is also negative, so that the surface is connected. This confirms our picture of a sponge-like structure for the bilayer membrane.

Anderson *et al.* [5] showed for periodic minimal surfaces of known area that the volume fraction of surfactant is related to the average mean curvature of the displaced surfaces *via*

$$\Phi^2 = \gamma l \langle H \rangle \frac{(3 - 2l \langle H \rangle)^2}{9(1 - l \langle H \rangle)^3} \quad (12)$$

where  $\gamma$  is in the range -2.25 to -1.7. (We now drop the subscripts on the average curvatures as they will from this point on always refer to the displaced parallel surfaces.) For weakly curved surfaces, equation (12) reduces to equation (3). We shall employ this approximation throughout this paper, and for simplicity take the value of  $\gamma$  to be -2. We shall also assume that, to a good approximation, equations (3) and (12) hold for the aperiodic minimal surfaces that are suitable models for the bilayer mid-surface of the L<sub>3</sub> phase [5].

To obtain the total free energy of the system, we must add the entropy of the disordered bilayer structure to the curvature free energy. The nature of the system is such that finding an exact expression for this quantity is a prohibitively difficult task. Previously Cates *et al.* [2] have developed a random mixing entropy expression in a cell model, leading to the entropy density scaling as  $s \sim \Phi^3$ . The same scaling argument developed by Porte *et al.* [3] to obtain the leading-order scaling of the total free energy density (Eq. (1)), also applies to the entropy density. The argument of Porte *et al.* is based on a truncation of the local curvature energy expansion at second order, as in equation (6). Then, dual configurations of the system, that is those differing only by a change of length scale, will have the same statistical weight when evaluating the Boltzmann average for the thermodynamic system. This leads to equation (1), and also applies equally well to the entropy density, so again  $s \sim \Phi^3$ .

As argued by Porte *et al.* [3], the sponge structure is formed due to a positive value of the saddle splay constant, resulting from a negative value of the spontaneous mean curvature of the constituent monolayers. A similar argument was made independently by Anderson *et al.* [5], who proposed that the sponge structure is then basically formed to match the monolayer spontaneous curvature. Entropic and fluctuation effects are secondary in comparison to this contribution. This should be compared to the lamellar phase, where they dominate the thermodynamics.

The suggestion of Porte *et al.* was that the observed sequence of phase transitions and narrowness of the sponge phase can be explained by considering the dependence of the Gaussian modulus (saddle splay constant) on the spontaneous curvature of the constituent monolayers; however they did not capture the commonly observed feature that the monolayer spontaneous curvature changes (which will be discussed in section 4) as the sponge is swollen. In this paper, the sequence of phase transitions, and finite swelling and narrow character of the sponge phase are successfully modelled, based upon the original suggestion of Anderson *et al.* [5] that the monolayer mean curvature energy dominates the free energy of the phase. Importantly, the monolayer spontaneous curvature is a varying parameter, rather than a fixed quantity, as the sponge is swollen.

With this in mind, we evaluate the free energy of the sponge phase, for the present, purely in terms of the average mean curvature contribution. We shall show that this allows us to capture all of the essential features of the phase observed experimentally in phase diagram studies, and further confirm the strength of this assumption through the results that we shall present later from light scattering. We do, however, bear in mind that contributions are present from fluctuations, Gaussian curvature and entropy, and these will be discussed in our concluding analysis.

Taking the first term on the r.h.s. of equation (8), expanding and employing equation (3) and using  $A/V = \Phi/l$  gives for the free energy density of the system

$$g = 2\kappa \left( \frac{H_0^2}{l} \Phi + \frac{H_0}{l^2} \Phi^3 + \frac{1}{4l^3} \Phi^5 \right) \quad (13)$$

The first term, linear in  $\Phi$ , can be absorbed into the standard chemical potential of the surfactant in the sponge phase. Its effect on the phase equilibrium between the sponge and the dilute solution is small compared to that of the difference in standard chemical potential of the surfactant in the monomeric state and in a free bilayer. Furthermore, we expect the same term to appear in the free energy expression for the lamellar phase, so the competition between the sponge and lamellar phases is also unaffected by this term. To an excellent approximation it can be ignored.

In equation (13), therefore, we have a free energy density expression of the form given in equation (2). The coefficient of the  $\Phi^3$  term in the free energy density is typically negative, whilst the coefficient of  $\Phi^5$  remains positive [16]. It is straightforward to calculate the chemical potentials of the surfactant (subscript s) and solvent (w):

$$\mu_s(L_3)/v_s = \mu_s^0(L_3)/v_s + 3a_3\Phi^2 - 2a_3\Phi^3 + 5a_5\Phi^4 - 4a_5\Phi^5 \quad (14)$$

and

$$\mu_w(L_3)/v_w = \mu_w^0/v_w - 2a_3\Phi^3 - 4a_5\Phi^5 \quad (15)$$

where  $a_3 = 2\kappa H_0/l^2$ ,  $a_5 = \kappa/(2l^3)$ ,  $v_s$  and  $v_w$  are the molecular volumes of the surfactant and solvent respectively, and  $\mu^0$  indicates a standard chemical potential.

### 3. The Competing Phases

As we have discussed previously, the sponge phase is usually observed to coexist with a dilute solution on one side of the single-phase region, and a lamellar phase on the other. In order to compute these phase equilibria, we give the free energies of these competing phases. Whilst equilibria with other phases, such as micellar, cubic and microemulsion phases are sometimes observed, we do not consider them as their contact with the sponge phase is marginal.

**3.1. THE DILUTE PHASE.** — We assume that only monomer surfactants are present in the dilute solution. The chemical potentials are readily derived in the dilute limit

$$\mu_s(L_1) = \mu_s^0(L_1) + k_B T \ln \left( \frac{v_w \Phi}{v_s} \right) \quad (16)$$

and

$$\mu_w(L_1) = \mu_w^0 - k_B T \frac{\Phi v_w}{v_s} \quad (17)$$

The standard chemical potential of the surfactant in solution is considerably larger than in the bilayer. Typical values for this difference  $\Delta\mu_s^0 = \mu_s^0(L_1) - \mu_s^0(L_3, L_\alpha)$  are in the range 10 - 25  $k_B T$  [17]. In comparison, the contribution from the term linear in  $\Phi$  in equation (13) to the difference in the standard chemical potentials is, for reasonable values of the spontaneous curvature, at least two orders of magnitude smaller.

**3.2. THE LAMELLAR PHASE.** — Helfrich [18] first calculated the free energy of the lamellar phase, which arises from the steric interaction of the undulating lamellar sheets. It is a simple step to generalize the Helfrich result to the specific case of bilayer sheets, so that the free energy density of the lamellar phase (excluding standard chemical potential terms) is given by

$$g = \frac{3\pi^2 (k_B T)^2 \Phi^3}{1024\kappa l^3} \quad (18)$$

Again, the chemical potentials are easily derived,

$$\mu_s(L_\alpha)/v_s = \mu_s^0(L_\alpha)/v_s + c(3\Phi^2 - 2\Phi^3) \quad (19)$$

and

$$\mu_w(L_\alpha)/v_w = \mu_w^0/v_w - 2c\Phi^3 \quad (20)$$

where  $c = 3\pi^2(k_B T)^2/(1024\kappa l^3)$ . The standard chemical potential of the surfactant is assumed to be the same as that in the sponge phase.

#### 4. Phase Diagram

Having obtained expressions for the free energies of the sponge phase, lamellar phase and dilute solution, we are now in a position to calculate the phase equilibria. This becomes a matter of equating the chemical potential of each component  $i$  at different compositions in each phase (phases m and n, say)

$$\mu_i(\Phi[m]) = \mu_i(\Phi[n]) \quad (21)$$

The nature of the expressions for the chemical potentials given in equations (14) to (17) and (19) and (20) means that this task requires the use of (uncomplicated) numerical techniques, and the insertion of some physical parameters into the calculation. Since the system that we study using light scattering is the pseudo-binary AOT- $\text{NaNO}_3$ -water system, it is useful at this stage to employ the values relevant to it. We take  $l = 9.5 \text{ \AA}$  [19],  $v_s = 639 \text{ \AA}^3$  [20],  $v_w = 30 \text{ \AA}^3$  and  $\Delta\mu_s^0 = 15\kappa_B T$ . The value of the bending modulus  $\kappa$  is less well known. In Figure 2a we show the calculated phase diagram using a value of  $\kappa = 2\kappa_B T$ , and in Figure 2b demonstrate the effect of increasing this value to  $5\kappa_B T$ .

It is evident that changes in both the spontaneous curvature and surfactant volume fraction induce phase transitions. In experimental systems, the spontaneous curvature can be tuned in various ways. For non-ionic surfactants [5, 6, 21] the spontaneous curvature is a strong function of temperature. In ionic surfactant systems, convenient tuning parameters are the salinity of the aqueous solvent [22], and in the presence of cosurfactant, the surfactant-to-cosurfactant ratio [3]. In both cases, the exact scaling of the spontaneous curvature to the controlling parameter (be it either temperature or salt concentration) is not known in general, and hence a qualitative, rather than a quantitative, comparison to experimental phase diagrams should be made.

We compare with the partial phase diagram which we have obtained for the pseudo-binary AOT- $\text{NaNO}_3$ -water system, presented in Figure 3. For the AOT- $\text{NaNO}_3$ -water system, the salt concentration becomes a controlling parameter, and induces phase transitions at fixed temperature. While we do not know the exact scaling of the spontaneous curvature of the membrane to the salt concentration, it is clear that increasing the latter quantity will cause the constituent monolayers to bend more towards the solvent. Hence increasing the salt concentration drives the spontaneous curvature to more negative values. As shown in Figure 3, the  $L_3$  phase appears to terminate at about 10%wt of AOT. The phase behaviour at lower surfactant concentrations is the subject of a continuing study, and has revealed interesting features, such as a small "island" of a single phase isotropic liquid, previously observed in other systems [23].

The first point to make about the calculated phase diagrams of Figure 2 is that they capture the essential features of the narrowness and finite swelling of the  $L_3$  phase, and the correct

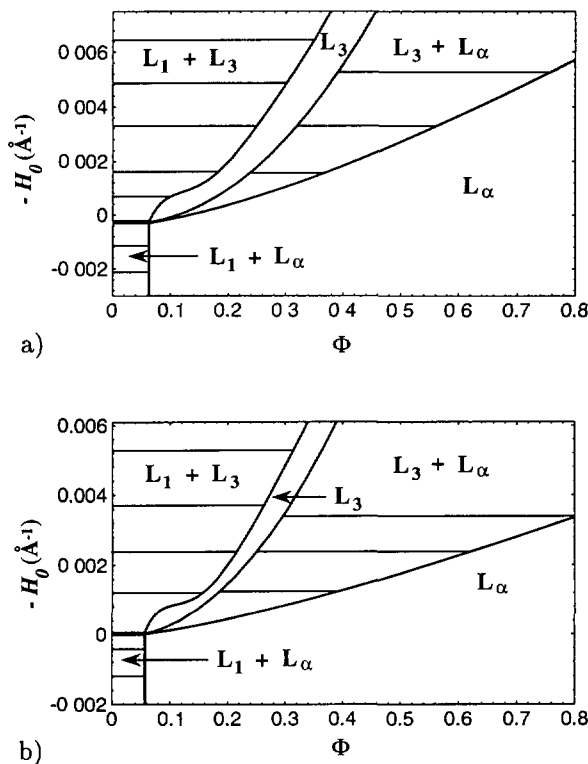


Fig. 2. — a) Phase diagram calculated from the model with  $\kappa = 2k_B T$ . The bold line indicates the three phase coexistence  $L_1/L_3/L_\alpha$ . b) Calculated phase diagram for  $\kappa = 5k_B T$ .

sequence of phase transitions in its vicinity, as experimentally observed (Fig. 3). Evidently, increasing the value of the bending modulus narrows the phase further, and broadens the two-phase coexistence region with lamellae. This is readily understood from the free energy densities of the two phases, equations (13) and (18). Increasing  $\kappa$  decreases the free energy of the lamellar phase at a given surfactant volume fraction, while making the free energy of the sponge more concentration-dependent, so that the lamellar phase is able to coexist with the sponge phase at lower surfactant volume fractions.

There is another parameter which may be altered. Although we do not show its effect here, the limits of maximum swelling, that is, the points at which the single-phase bilayer regions terminate at the dilute end, are sensitive to the value of  $\Delta\mu_s^0$ . Decreasing this value causes the sponge and lamellar phases to terminate at a higher surfactant concentration. It is difficult, however, to give a definitive value for this difference in the standard chemical potential of the surfactant in the dilute and bilayer phases. It is important to note, though, that the limits of maximum swelling seem to be controlled by this parameter.

Looking more closely at the calculated phase diagrams, the broad line adjacent to the dilute end of the single-phase  $L_3$  region corresponds to a three-phase coexistence line of dilute solution, sponge and lamellae. Below the three-phase line, there is a small two-phase region of dilute solution and lamellar phase. At the dilute end, the two-phase coexistence between the sponge and lamellar phases is becoming narrow. In fact, the limits of maximum swelling for the sponge and lamellar phases are at almost identically the same point. There is also an extremely narrow

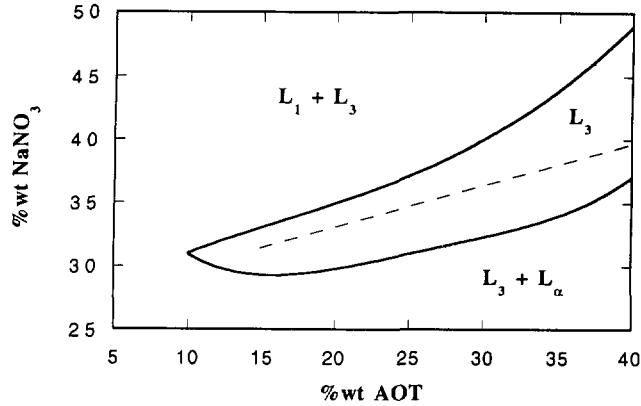


Fig. 3. — Partial phase diagram for the AOT-NaNO<sub>3</sub>-water system at 23 °C. The line within the phase is the third dilution line used for the light scattering experiments.

(from  $\Phi = 0$  to about  $10^{-6}$ ) single-phase  $L_1$  region not shown on the phase diagrams due to its size.

Another point to be made is that at the dilute end, the sponge phase is stable even for positive spontaneous curvatures, over a very small range of values. This can be understood again from the free energy density expressions (13) and (18). For very small and positive values of the spontaneous curvature, and at high dilution where the quintic term in the sponge free energy density is not significant, the sponge phase will still be able to successfully compete with lamellae due to its smaller free energy. Under dilution, one expects the spontaneous curvature of the sponge membrane to become less negative as it swells, and within the assumptions of our model, at a certain point it undergoes a change of sign, and the constituent monolayers bend away from the solvent for a small range of surfactant volume fractions.

So, we have seen that the calculated phase diagrams from the proposed model successfully reproduce the important experimentally observed features of the sponge phase and its nearby phases. We have demonstrated, for the first time, a mechanism which readily accounts for the narrowness and finite swelling of the phase, with the monolayer spontaneous curvature as a controlling parameter, rather than a fixed constant, as the sponge is swollen. The original hypothesis [5, 6] that the bending energy of the average mean curvature dominates the thermodynamics of phases such as the sponge seems a sound one indeed.

## 5. Light Scattering

Having tested the model in terms of phase behaviour, we seek further evidence for its validity from static light scattering experiments. This is an excellent technique for doing so, as we can relate a calculated quantity, the osmotic pressure  $\Pi$ , to an experimentally determined quantity, the absolute forward scattering intensity, i.e. the excess Rayleigh ratio  $\Delta R(q)$  extrapolated to  $q = 0$  [24, 25]

$$\Delta R(0) = \frac{4\pi^2 n_0^2}{\lambda_0^4} \left( \frac{dn}{d\Phi} \right)^2 k_B T \Phi \left( \frac{\partial \Pi}{\partial \Phi} \right)^{-1} \quad (22)$$

where  $n_0$  is the refractive index of the solvent,  $n$  is the refractive index of the solution, and  $\lambda_0$  is the wavelength of the incident light in vacuum [26]. The osmotic pressure can be obtained

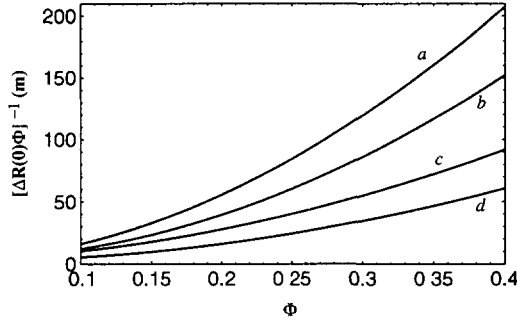


Fig. 4. — Plot of  $[\Delta R(0)\Phi]^{-1}$  vs.  $\Phi$  calculated from the model for  $\kappa = 2k_B T$  and  $\kappa = 5k_B T$ . The curves correspond to the following predictions: a, along  $L_3/L_\alpha$  phase boundary,  $\kappa = 5k_B T$ ; b, along  $L_3/L_1$  phase boundary,  $\kappa = 5k_B T$ ; c, along  $L_3/L_\alpha$  phase boundary,  $\kappa = 2k_B T$ ; d, along  $L_3/L_1$  phase boundary,  $\kappa = 2k_B T$ .

directly from equation (15) *via*

$$\Pi = -\mu_w(L_3)/v_w \quad (23)$$

Now, it is of the utmost importance to *specify the dilution line* within the phase along which a prediction is made for the forward scattering intensity, as this quantity is dependent on both the salt concentration and the volume fraction of surfactant in a system such as AOT-NaNO<sub>3</sub>-water. The same dilution line must then be followed experimentally if confirmation of this prediction is sought. In our view, previous light scattering studies of sponge phases have suffered from not specifying dilution lines.

If we were to calculate the expected scattering intensity from the first-order scaling law of equation (1), then we would expect the scaling form

$$\Delta R(0) \sim \Phi^{-1} \quad (24)$$

Previous studies [9-11] have indicated a deviation away from this first-order scaling, and the interpretation has been a logarithmic correction due to renormalization of the bending constants, deriving from the ACRS free energy density form of equation (5), so that

$$[\Delta R(0)]^{-1} \sim \Phi(r_1 + r_2 \ln \Phi) \quad (25)$$

Clearly, our model will make a different prediction for the scattering intensity scaling.

In Figure 4 we show the (numerically) calculated scattering intensities from the model for  $\kappa = 2k_B T$  and  $5k_B T$ . These are plotted as  $[\Delta R(0)\Phi]^{-1}$  vs.  $\Phi$ . Curves a and c represent the predictions along the  $L_3/L_\alpha$  phase boundary, and b and d that along the  $L_3/L_1$  phase boundary. All of these curves are excellently approximated by quadratics, so that

$$[\Delta R(0)]^{-1} \approx d_3 \Phi^3 + d_2 \Phi^2 + d_1 \Phi \quad (26)$$

over the range of volume fractions indicated on the graphs. Values of the coefficients  $d_j$  for the curves appearing in Figure 4 are given in Table I. Importantly, we predict a *significant change in the scattering intensity in moving from one phase boundary to the other at constant surfactant volume fraction*. This can be understood from thermodynamic considerations, as the narrow character of the phase means that the free energy density is a rapidly changing function

Table I. — Values for the coefficients  $d_j$  of equation (26). The first six rows correspond to values calculated from the model along the L<sub>3</sub>/L<sub>α</sub> and L<sub>3</sub>/L<sub>1</sub> phase boundary dilution lines, with  $\kappa = 2k_B T$ ,  $\kappa = 5k_B T$  and  $\kappa = 1.8k_B T$ , the latter giving good agreement with the experimental results which are presented in the last two rows. Note that the value of the coefficient  $d_2$  is less well-determined than the other two, as the quadratic term in equation (26) is less significant than either the cubic or linear terms over the range of surfactant volume fractions considered.

Dilution line	$d_3$ (m)	$d_2$ (m)	$d_1$ (m)
L <sub>3</sub> /L <sub>α</sub> phase boundary, $\kappa = 2k_B T$	494	24.9	3.04
L <sub>3</sub> /L <sub>1</sub> phase boundary, $\kappa = 2k_B T$	392	-12.2	2.87
L <sub>3</sub> /L <sub>α</sub> phase boundary, $\kappa = 5k_B T$	1214	30.4	1.00
L <sub>3</sub> /L <sub>1</sub> phase boundary, $\kappa = 5k_B T$	970	-19.2	4.47
L <sub>3</sub> /L <sub>α</sub> phase boundary, $\kappa = 1.8k_B T$	449	22.6	3.53
L <sub>3</sub> /L <sub>1</sub> phase boundary, $\kappa = 1.8k_B T$	353	-11.3	2.65
L <sub>3</sub> /L <sub>α</sub> phase boundary, experimental results	465	-28.2	18.0
L <sub>3</sub> /L <sub>1</sub> phase boundary, experimental results	333	-31.1	13.3

of both the concentration and spontaneous curvature; hence there will be a large variation in the compressibility in moving across the phase. The measurements taken in order to test this prediction were therefore made along three dilution lines: two as near as possible to the phase boundaries, and another well within the phase as indicated in the phase diagram of Figure 3. The latter was done to further test the prediction of the salt concentration dependency of the forward scattering intensity.

5.1. MATERIALS AND METHODS. — The surfactant, sodium bis(2-ethylhexyl) sulfosuccinate (AOT) was obtained from Sigma and used without further purification. Sodium nitrate (99%) was obtained from Merck, and millipore water was used.

Samples were prepared in sealed tubes, vortex-mixed, and allowed to equilibrate over (at least) one day. Phase diagram determination was done by visual inspection, between cross-polarisers when necessary. Static light scattering experiments were performed with a commercially available Malvern 4700 PS/MW spectrometer equipped with a computer-controlled, stepping-motor-driven goniometer, a digital correlator (Malvern, Model 7032-ES/136c), and an argon laser (Coherent, Innova 200-10,  $\lambda_0 = 488$  nm). The measurements were performed at  $23.0 \pm 0.1$  °C. Approximately 1 ml of solution was transferred into the cylindrical scattering cell. The cell was then sealed and centrifuged for 45-120 min at approximately 6000g and 23 °C

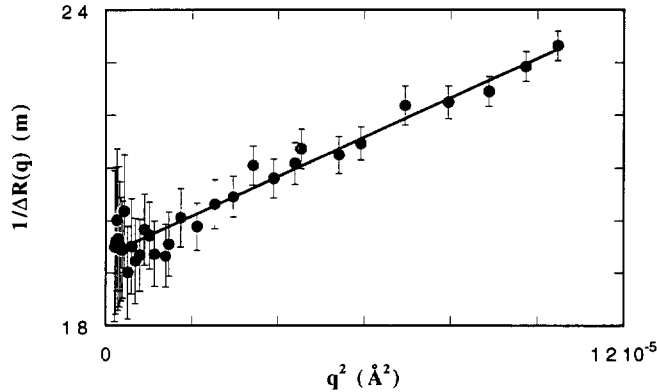


Fig. 5. — A plot of the  $q$ -dependence of  $\Delta R(q)$ . This one is for a sample of volume fraction  $\Phi = 0.1354$ . The line of best fit is shown.

in order to remove dust particles from the scattering volume.

The static light scattering experiments were performed at 13 different angles ( $30^\circ \leq \theta \leq 150^\circ$ ) and 60 individual measurements were taken and averaged for each angle, thus yielding the average scattering intensity  $\langle I_s(\theta) \rangle$ . The data were then converted to excess Rayleigh ratios using [27]

$$\Delta R(q) = \frac{\langle I_s(q) \rangle}{\langle I_{\text{ref}}(q) \rangle} R_{\text{ref}}(q) \left( \frac{n}{n_{\text{ref}}} \right)^2 \quad (27)$$

where  $R_{\text{ref}}(q) = 3.96 \times 10^{-3} \text{m}^{-1}$  is the Rayleigh ratio and  $n_{\text{ref}} = 1.499$  the refractive index of the reference solvent toluene. The other parameters relevant to equations (22) and (27) are  $n_0 = 1.34$  and  $dn/d\Phi = 0.14$ , the latter quantity obtained in the approximation that the refractive index of the solution has a linear  $\Phi$ -dependence over the chosen range of surfactant volume fractions. We have taken the refractive index of AOT to be 1.48 [28].

We have examined the  $q$ -dependence of the scattering intensity for the most dilute sample in more detail, as shown in Figure 5. As is seen, it can be described by a simple Ornstein-Zernike form  $\Delta R(q) = A/(1 + Bq^2)$ . Deviations away from this form could have possibly been expected for the more dilute samples as here the correlation length is longest, however as Figure 5 shows, we did not observe any such deviations. This facilitates, and minimizes the error in, the extrapolation for the evaluation of  $\Delta R(0)$ .

5.2. RESULTS. — The measurements obtained from the static light scattering experiments are presented in Figure 6. The solid curves are polynomials of best fit to the data for the  $L_3/L_\alpha$  phase boundary dilution line (upper curve) and the  $L_3/L_1$  phase boundary dilution line (lower curve). The results for the dilution line well within the phase are represented by open triangles. Also shown by dashed curves are the predictions from the model using  $\kappa = 1.8k_B T$ , the value of the monolayer bending modulus which gives good agreement with the experimental results.

The data for the dilution lines along the phase boundaries are excellently fitted by quadratics (the coefficients given in Table I), suggesting that the functional form for the forward scattering intensity is that which we predicted from the model in equation (26). The only parameter which we have adjusted to compare the predictions of the model with the experimental results is  $\kappa$ , and *on an absolute scale* we see very good agreement. The minor discrepancies between the predicted and observed results could be explained by the missing contributions of fluctuations,

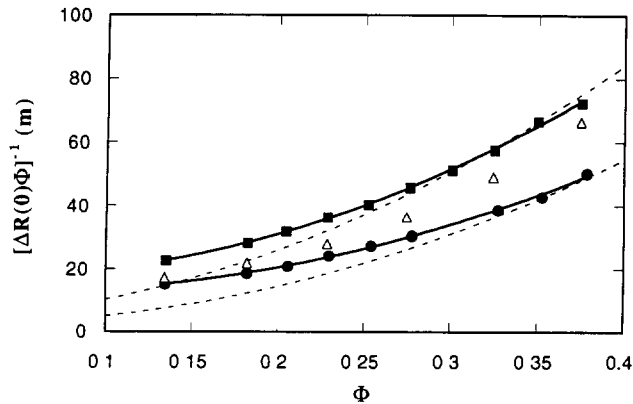


Fig. 6. — The results of the static light scattering experiments. The squares correspond to the results along the  $L_3/L_\alpha$  phase boundary dilution line, the circles to those along the  $L_3/L_1$  phase boundary, and the triangles to the dilution line well within the phase (see Fig. 3). Both solid curves are quadratics of best fit. Dashed curves correspond to the predictions from the model for  $\kappa = 1.8k_B T$ .

entropy and Gaussian curvature. In any case, it is clear that including only the average mean curvature contribution to the free energy allows us to successfully make a quantitative prediction for the forward scattering intensity as a function of surfactant volume fraction. Having only one free parameter in the model also allows us to make a prediction for the bending modulus of the AOT bilayer

$$\kappa_{\text{bilayer}} = 2\kappa \approx 3.6k_B T \quad (28)$$

So, what we have shown is that the model predicts the scattering intensity along the phase boundaries of the sponge phase. It also correctly predicts a significant increase in the scattering intensity at constant surfactant volume fraction when the salt concentration is increased, reinforcing the notion that a clear specification of the dilution line when using light scattering experiments to test models of the sponge phase is crucial. The results strongly support the argument that it is the average mean curvature which dominates the thermodynamics of the phase.

Finally, no logarithmic correction to the scattering intensity scaling of the form given in equation (25) is seen in these results. To confirm this, in Figure 7 we have plotted  $[\Delta R(0)\Phi]^{-1}$  vs.  $\ln \Phi$ . On such a plot, equation (25) would predict a linear relationship, and this is clearly not the observed result.

## 6. Discussion

The conclusion that we drew in the previous section, that we find no evidence for a logarithmic correction to the scaling law for  $\Delta R(0)$ , is in clear disagreement with previous studies [9-11]. What are the possible reasons for this disagreement? In some cases, the previous experiments have been performed on quaternary systems (surfactant, brine, oil and cosurfactant). These systems have been the subject of related discussions regarding the possibility of critical points appearing in the phase, such as the mooted symmetric to asymmetric sponge second-order phase transition [29, 30]. These issues remain the subject of strong debate [31]. Clearly, the presence of such critical points will have a strong effect on scattering data. Avoiding this

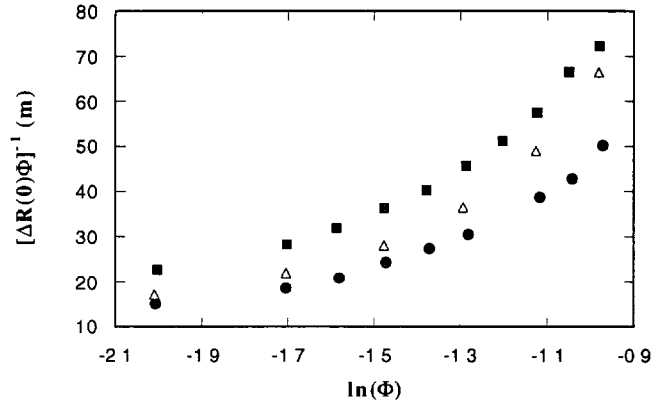


Fig. 7. — The results of Figure 6 plotted as  $[\Delta R(0)\Phi]^{-1}$  vs.  $\ln \Phi$ . Clearly, the relationship is not linear along any dilution line.

complication is a good motivation for using a pseudo-binary system, where no such critical points have been observed, to test the model. In fact, the scattering data of Figure 6 indicates an absence of critical points of any kind in the region of our investigation.

Whilst not wishing to belabour the point, if the dilution line within the phase is not specified, then in principle one could deduce a myriad of functional forms for the scattering intensity, simply by altering the dilution line. This is clear from our experimental results, particularly if one considers the data obtained from the line well within the phase. It is only with a careful specification of the dilution line that *any* conclusions can be drawn about the scaling of the forward scattering intensity.

Finally on this issue, we note, as outlined throughout this paper, that we have strong reason to believe that the logarithmic term does not appear in the free energy of the sponge phase, based upon the theoretical arguments presented originally in reference [4]. The experimental data that we have obtained in support of that notion extends over the region  $\Phi = 0.13 - 0.38$ . This is a constraint imposed by the particular system chosen for the study. A future aim is to further test the notion in the more dilute regime with another system, with the same criterion of careful dilution-line specification. One definitive point can be made at this stage, however: we have given strong proof from the light scattering experiments for the existence of the quintic correction to the free energy density originally proposed in reference [4] over the range of surfactant volume fractions considered. Moreover, the model remains successful in describing the nature of the phase diagram well into the very dilute regime, in fact (referring to Fig. 2) to surfactant volume fractions of about 0.05. That is, we have shown that the logarithmic correction to the free energy is unnecessary in describing any of the observed features of the phase diagram, and that a free energy density of the generic form given in equation (2) is *sufficient over all concentration regimes* for doing so.

We turn now to the promised discussion on the effects of fluctuations, Gaussian curvature and entropy. Taking the last of these first, we have already argued that the entropy density has a cubic scaling with  $\Phi$ . We may also apply those arguments to the scaling of the fluctuation contribution to the free energy density, giving the same leading-order scaling form. As Pieruschka *et al.* [8] have shown for the case of lamellae, there is also a  $\Phi^5$  correction to this contribution in an expansion to higher orders. More can also be said about the Gaussian curvature. There is a correction from ideal scaling for average Gaussian curvature density con-

tribution to the free energy. This comes from the finite thickness of the monolayers composing the bilayer. The average Gaussian curvature per unit cell of a bilayer structure modelled by a periodic minimal surface is  $\langle K \rangle_u / \alpha^3$ , where  $\alpha$  is the ‘‘lattice parameter’’ of the structure. The lattice parameter can be related to the volume fraction of surfactant *via* [32]

$$\Phi = \frac{2\mathcal{C}l}{\alpha} \left[ 1 + \frac{2\pi\chi_E}{\mathcal{C}} \left( \frac{l}{\alpha} \right)^2 \right] \quad (29)$$

where  $\mathcal{C}$  is a (positive) dimensionless area-scaling constant given by the particular structure of the sponge. Again, we assume that this applies approximately to the aperiodic minimal surfaces appropriate to the L<sub>3</sub> phase. Inverting this equation in the limit of small volume fractions gives

$$\langle K \rangle / V = \langle K \rangle_u / \alpha^3 = \frac{\langle K \rangle_u \Phi^3}{8\mathcal{C}^3 l^3} \left( 1 - \frac{3\pi\chi_E}{2\mathcal{C}^3} \Phi^2 \right) \quad (30)$$

Therefore we have a quintic correction to ideal scaling. Hence we see nothing that will alter the *qualitative* behaviour of the free energy density if we were to include fluctuations, Gaussian curvature and entropy. The scaling law would still be of the form given in equation (2), and none of the major conclusions that we have drawn so far would be altered. The fact that so many of the observed experimental features of the phase diagram and scattering data are captured by including only the average mean curvature contribution to the sponge free energy indicates that these other effects are indeed secondary, and that the average mean curvature is the important quantity in determining the behaviour of the phase.

## 7. Conclusion

In this paper, we have developed a model which we believe successfully accounts for the experimentally observed features of the L<sub>3</sub> (sponge) phase: its finite swelling and narrowness, the observed sequence of phase transitions in its vicinity, and its light scattering behaviour. We have predicted and shown experimentally with regards to the latter how the forward scattering intensity varies with salt concentration for the pseudo-binary system AOT-NaNO<sub>3</sub>-water, and emphasized the importance of specifying a dilution line within the phase when using light scattering to test the model. The hypothesis that average mean curvature is the quantity that controls the behaviour of the phase appears to be correct. Finally, the experimental results indicate, over the range of surfactant volume fractions considered ( $\Phi = 0.13 - 0.38$ ), that there is no evidence for the appearance of the logarithmic correction to the free energy, previously suggested by others to arise from renormalisation of the bending constants.

## Acknowledgments

We thank Plamen Petrov, Andrew Fogden, Alexey Kabalnov and Marc Leaver for valuable discussions. J.D. thanks Peter Schurtenberger and his group at the ETH in Zürich for their hospitality during the course of the light scattering experiments. This work was supported by the Swedish Natural Science Research Council (NFR).

## References

- [1] Fontell K., In Colloidal Dispersions and Micellar Behaviour, ACS Symposium Series No. 9 (American Chemical Society, Washington D.C., 1975) p. 270.
- [2] Cates M. E., Roux D., Andelman D., Milner S. T., Safran S. A., *Europhys. Lett.* **5** (1988) 733.
- [3] Porte G., Appell J., Bassereau P., Marignan L., *J. Phys France* **50** (1989) 1335.
- [4] Wennerström H., Olsson U., *Langmuir* **9** (1993) 365.
- [5] Anderson D., Wennerström H., Olsson U., *J. Phys Chem* **93** (1989) 4243.
- [6] Olsson U., Wenneström H., *Adv. Colloid Interface Sci.* **49** (1994) 113.
- [7] Andelman D., Cates M. E., Roux D., Safran S. A., *J. Chem Phys* **87** (1987) 7229.
- [8] Pieruschka P., Marcelja S., Teubner M., *J. Phys. II France* **4** (1994) 763.
- [9] Porte G., Delsant M., Billard I., Skouri M., Appell J., Marignan J., Debeauvais F., *J Phys. France II* **1** (1991) 1101
- [10] Skouri M., Marignan J., Appell J., Porte G., *J. Phys. II France* **1** (1991) 1121.
- [11] Roux D., Cates M. E., Olsson U., Ball R. C., Nallet F., Bellocq A. M., *Europhys. Lett.* **11** (1990) 229.
- [12] Helfrich W., *Z. Naturforsch.* **28c** (1973) 693.
- [13] Wennerström H., Anderson D. M., In Statistical Mechanics and Differential Geometry of Micro-Structured Materials, A. Friedman, J. C. C. Nitsche and H. T. Davis Eds. (Springer Verlag, Berlin, 1991).
- [14] David F., In Statistical Mechanics of Membranes and Surfaces, D. Nelson, T. Piran and S. Weinberg Eds. (World Scientific, Singapore, 1989).
- [15] Weatherburn C., *Differential Geometry of Three Dimensions* (Cambridge University Press: Cambridge, 1926).
- [16] In principle, there is also a quintic contribution to the free energy density from an expansion to the next order in the local monolayer curvature energy of equation (6). Since there is no direct way of characterizing the coupling constant for this term, we do not include this contribution to the free energy density. The validity of this omission is seen *post facto* from the good agreement we obtain between the model and the light scattering data by only keeping the contribution to the quintic term in the free energy density from the harmonic leading-order term of the local monolayer curvature energy (see Sect. 5).
- [17] Tanford C., *The Hydrophobic Effect: Formation of Micelles and Biological Membranes* (Wiley, New York, 1980).
- [18] Helfrich W., *Z. Naturforsch.* **33a** (1978) 305.
- [19] Strey R., Jahn W., Skouri M., Porte G., Marignan J., Olsson U., In Structure and Dynamics of Strongly Interacting Colloids and Supramolecular Aggregates in Solution, S. Chen, J. S. Huang and P. Tartaglia Eds. (Kluwer Academic Publishers, Dordrecht, the Netherlands, 1992) p. 351.
- [20] Fontell K., *J. Colloid Interface Sci.* **44** (1973) 318
- [21] Strey R., *Colloid Polym. Sci.* **272** (1994) 1005
- [22] Olsson U., Strom P., Söderman O., Wennerström H., *J Phys. Chem.* **93** (1989) 4572.
- [23] Bellocq A. M., Roux D., In Microemulsions: Structure and Dynamics, S. E. Friberg and P. Bothorel Eds. (CRC press, 1987).
- [24] Schurtenberger P., Newman M. E., In Characterization of Environmental Particles, J. Buffle and H. T. v. Leeuwen Eds., Vol. 2 (Lewis Publishers, 1993) p. 37.
- [25] Candau S J., In Surfactant Solutions New Methods of Investigation., R. Zana Ed. (Marcel Dekker, New York, 1987) p. 147.
- [26] We note that this formulation is strictly correct only for binary systems. In our study (as for many previous to ours), we have used a pseudo-binary system: therefore the assumption is that the brine is a pseudo-component, and that this standard formula relating the scattering intensity to the osmotic compressibility still applies, at least to a very good approximation.

- [27] Olsson U., Schurtenberger P., *Langmuir* **9** (1993) 3389.
- [28] Ricka J., Borkovec M., Hofmeier U., *J. Chem. Phys.* **94** (1991) 8503.
- [29] Coulon C., Roux D., Bellocq A. M., *Phys. Rev. Lett.* **66** (1991) 1709.
- [30] Roux D., Coulon C., Cates M. E., *J. Phys. Chem.* **96** (1992) 4174.
- [31] Filali M., Porte G., Appell J., Pfeuty P., *J. Phys. II France* **4** (1994) 349.
- [32] Anderson D. M., Davis H. T., Scriven L. E., Nitsche J. C. C., *Adv. Chem. Phys.* **77** (1990) 337.